

Temperature dependence of Fe,Mg partitioning in Acapulco olivine

ROLF HEINEMANN,¹ VERONIKA STAACK,¹ ARNE FISCHER,¹
HERBERT KROLL,^{1,*} THOMAS VAD,² AND ARMIN KIRFEL³

¹Institut für Mineralogie, Westfälische Wilhelms-Universität, Corrensstrasse 24, D-48149 Münster, Germany

²Mineralogisches Institut, Universität Würzburg, Am Hubland, D-97074 Würzburg, Germany

³Mineralogisch-Petrologisches Institut, Universität Bonn, Poppelsdorfer Schloss, D-53115 Bonn, Germany

ABSTRACT

The temperature dependence of the intracrystalline Fe,Mg partitioning (K_D) in two olivine crystals (Fa_{11}) separated from the Acapulco meteorite was determined by single-crystal X-ray structure analysis. The independent atom model (IAM) was compared with a “bond model” which accounts for bond-induced charge accumulations on the Si-O bonds. Outliers in the set of structure amplitudes observed when using the IAM disappeared upon introducing the bond model. The crystals were equilibrated at 750, 650, and 500 °C. The refined site occupancies yield the relation $\ln(K_D) = 0.345(60) - 204(53)/T$, where T is in K, which is in qualitative agreement with earlier work. Comparison of these data with the higher temperature data of Artioli et al. (1995) suggests an unusual temperature variation of the Fe,Mg distribution within two temperature regimes. Below 880 °C, Fe tends to order onto the M1 site with increasing temperature whereas it concentrates on the M2 site above 880 °C. In principle, olivine may serve as a geospeedometer similar to orthopyroxene. However, at present its usefulness is restricted because (1) the relatively weak dependence of $\ln(K_D)$ on temperature needs to be even more tightly constrained than presented here and (2) low-temperature extrapolation of the rate constants for the Fe,Mg site exchange, derived from interdiffusion coefficients, is uncertain.

INTRODUCTION

The temperature dependent distribution of Fe and Mg on the non-equivalent M1 and M2 sites of olivines, $(Mg,Fe)_2[SiO_4]$, is characterized by a weak tendency of Fe to order onto the M1 site with increasing temperature (e.g., Aikawa et al. 1985; Ottonello et al. 1990; Princivalle 1990). Because it is difficult to quench equilibrium states from above 800–900 °C, Artioli et al. (1995) and Rinaldi et al. (1997) performed in situ neutron diffraction experiments from which they infer that at high temperatures Fe no longer prefers M1, but concentrates in M2.

Kirfel (1996) performed a round robin in which various laboratories were asked to refine Fe,Mg distributions in orthopyroxenes and olivines from X-ray intensity data provided by that author. The large spread of the returned results was disconcerting. The same olivine, for example, was reported with Fe preferring M1 or M2, respectively, depending on the laboratory.

In the following, we report on Fe,Mg ordering states derived from refinement techniques which are considered to reduce the inadequacy of the conventional independent atom model (IAM) with respect to modeling bond-induced charge redistributions. Two olivine crystals from the Acapulco meteorite (Fa_{11}) were equilibrated at 750, 650, and 500 °C, then quenched to room temperature, and their site occupancies refined from X-ray intensities.

EXPERIMENTAL METHODS

Microprobe analysis

Several olivine crystals were kindly provided by J. Zipfel, Mainz. Two of them were selected for X-ray single crystal work. They were optically clear and exhibited sharp optical extinctions and sharp singular spots in Laue photographs. Two other crystals less suitable for X-ray single crystal studies but free of inclusions were analyzed with a JEOL Superprobe (JXA-8600 MX). The data were reduced by a ZAF correction. The crystals proved to be homogeneous and compositionally identical within error limits. Mean values of 203 point analyses with weight percentages between 98.5 and 101.5% are given in Table 1 along with the results of Zipfel et al. (1995) demonstrating excellent agreement.

Heat treatment

After collecting their X-ray intensity data the two selected crystals were heat-treated. Each crystal was placed in a SiO₂-glass capillary. Then, both capillaries were loaded side by side into a SiO₂-glass capsule together with Fe powder separated from the capillaries. The capsule was repeatedly evacuated, filled with purified Ne, and finally sealed. The crystals were annealed at 750 °C for 4 days, and then, after rapid quenching into water, analyzed by X-ray diffraction. This procedure of heating, quenching, and subsequent X-ray analysis was repeated for temperatures of 650 and 500 °C, allowing equilibration times of 6 and 26 days, respectively.

*E-mail: kroll@nwz.uni-muenster.de

TABLE 1. Electron microprobe analyses of Acapulco olivines

This work				Zipfel et al. (1995)				
oxide	weight%	cation	a.p.f.u.	oxide	weight%	cation	a.p.f.u.	a.p.f.u. (adj.)
SiO ₂	40.61(31)	Si	1.009(5)	SiO ₂	40.29	Si	1.005	1.000
MgO	47.19(21)	Mg	1.748(8)	MgO	47.06	Mg	1.751	1.760
FeO	10.71(21)	Fe	0.222(4)	FeO	11.00	Fe	0.229	0.230
MnO	0.55(5)	Mn	0.015(1)	MnO	0.55	Mn	0.010	0.010
CaO	0.01(1)	Ca	0	CaO	–	Ca	–	–
NiO	0.01(2)	Ni	0	NiO	–	Ni	–	–
Sum	99.09(41)		2.994(18)		98.89		2.995	3.000

RATE CONSTANTS AND Fe,Mg INTERDIFFUSION COEFFICIENTS

The Fe,Mg exchange between M1 and M2 is very fast at high temperatures (Akamatsu and Kumazawa 1993). Therefore, one must be certain that quenching from 750 °C was fast enough to preserve the attained equilibrium distribution. Likewise, it needed to be confirmed that the annealing time at 500 °C was sufficiently long to achieve equilibrium.

Time constants for equilibration can be found from rate constants for the Fe,Mg site exchange. However, rate constants for olivine have not yet been determined. As an alternative, we will estimate them from the temperature variation of the Fe,Mg interdiffusion coefficient \tilde{D} (Bocquet et al. 1983; Akamatsu and Kumazawa 1993; Ganguly and Tazzoli 1994). Following the notation of Bocquet et al. (1983), the coefficient of diffusion \tilde{D} along a specific direction \vec{x} is related to atomic jump frequencies by

$$\tilde{D}_x = \frac{1}{2} \sum_{k=1}^z \Gamma_k x_k^2, \quad (1)$$

where z is the number of jump directions, Γ_k the mean atomic jump frequency for the k -th direction, and x_k the displacement of a k -jump projected onto the \vec{x} -direction. In olivine, each M1 octahedron has six neighboring M2 octahedra, and vice versa, i.e., $z = 6$. The M1-M2 vectors have an average component $x_k = b/4$ along the b -direction, which is the one direction where only jumps between M1 and M2 contribute to diffusion. Then Equation 1 reads

$$\tilde{D}_b = \frac{1}{2} \left(\frac{b}{4} \right)^2 \sum_{k=1}^6 \Gamma_k. \quad (2)$$

Following Ganguly and Tazzoli (1994), the jump frequency sum, $\Sigma \Gamma_k$ may be related to the rate constants of the chemical rate equation of Mueller (1967, 1969):

$$\frac{d(X_{\text{Fe}}^{\text{M2}} - X_{\text{Fe}}^{\text{M1}})}{dt} = -k_{21} X_{\text{Fe}}^{\text{M2}} X_{\text{Mg}}^{\text{M1}} + k_{12} X_{\text{Fe}}^{\text{M1}} X_{\text{Mg}}^{\text{M2}} \quad (3)$$

where X_i^α are site occupancies of species i on site α , k_{21} is the rate constant for Fe(M2→M1) or Mg(M1→M2) exchanges, and similarly k_{12} is the rate constant for Mg(M2→M1) or Fe(M1→M2) exchanges. Thus, k_{21} may be equated with the number of jumps per unit time that an Fe atom performs between an M2 site and the six adjacent M1 sites, and similarly k_{12} may be equated with the number of jumps per unit time that an Mg atom performs between an M2 site and the six adjacent M1 sites. Then, the total number of jumps per unit time that occur between an M2 site and the six M1 neighbors, or equivalently between an M1 site and the six M2 neighbors, is $k_{21} + k_{12} = \Sigma \Gamma_k$, and therefore

$$\tilde{D}_b = \frac{k_{21} + k_{12}}{2} \left(\frac{b}{4} \right)^2. \quad (4)$$

Equation 4 corresponds to Equation 6 of Ganguly and Tazzoli (1994), except that the average jump projection on b enters rather than the mean M1-M2 distance itself. Given that $K_D = k_{21}/k_{12}$, Equation 4 can be transformed into

$$k_{21} = \frac{2\tilde{D}_b}{(b/4)^2} \left(\frac{K_D}{1 + K_D} \right). \quad (5)$$

Diffusion coefficients in olivine have been measured by Buening and Buseck (1973), Misener (1974), Jurewicz and Watson (1988), and most recently by Chakraborty (1997) who determined \tilde{D}_c in experiments between 1300 and 980 °C. Further experiments at lower temperatures, which were evaluated by TEM techniques, showed agreement with diffusion coefficients obtained by extrapolation of the high temperature results Chakraborty (personal communication). Chakraborty (1997) gives reasons why the results of Buening and Buseck (1973) and to some extent those of Misener (1974) differ from his. In addition, his experimental setup avoids shortcomings of the earlier work. Hence, we consider Chakraborty's (1997) results to be more reliable.

Diffusion in olivine is anisotropic. Because Chakraborty measured \tilde{D}_c rather than \tilde{D}_b we have to relate \tilde{D}_b to \tilde{D}_c . At high temperatures it is found that $\tilde{D}_c/\tilde{D}_b \approx 5$, but this ratio increases with decreasing temperature according to Buening and Buseck (1973) and Misener (1974). The results of Jurewicz and Watson (1988), however, do not support this view. For the time being we will assume that $\tilde{D}_c/\tilde{D}_b = 5$, being aware that this may be an oversimplification.

Diffusion coefficients in olivine also depend on oxygen fugacity. Chakraborty (1997) determined at \tilde{D}_c constant fugacity, $f_{\text{O}_2} = 10^{-12}$ bar. Following Buening and Buseck (1973)

$$\ln \tilde{D}(f_{\text{O}_2}) = \ln \tilde{D}(f_{\text{O}_2} = 10^{-12} \text{ bar}) + 0.167 \ln \frac{f_{\text{O}_2}(T)}{10^{-12}}. \quad (6)$$

The question is, below which temperature does the diffusion coefficient become independent of f_{O_2} ? Chakraborty (1997) argues that at low temperatures, in the pure extrinsic diffusion regime (roughly below 800 °C, personal communication), diffusion rates become independent of oxygen fugacity because in that region impurity defects represent the majority of point defects.

Accepting a constant $\tilde{D}_c/\tilde{D}_b = 5$ and an oxygen fugacity correction at 800 °C according to the iron-wüstite buffer, leads to an Arrhenius relation for k_{21} :

$$k_{21} (\text{d}^{-1}) = 1.23 \cdot 10^{14} \exp[-54.2(\text{kcal/mol})/RT] \quad (7)$$

where R is the gas constant.

The time constants for equilibration, roughly approximated by k_2^{-1} and calculated from Equation 7, would be 4 min at 750 °C and 17 d at 500 °C. Thus, they would both be sufficiently large to successfully quench the site distribution from 750 °C, and sufficiently short to ensure that equilibrium was reached within 26 d at 500 °C, respectively.

X-RAY STRUCTURE ANALYSIS

Data collection and reduction

Intensity data were collected in four or eight *hkl*-octants, up to $\sin\theta/\lambda = 1.1 \text{ \AA}^{-1}$ using $\theta/2\theta$ scans. On average, 1265 unique reflections with $|F_o| > 3\sigma$ were obtained. Absorption effects were corrected applying the semi-empirical method of North et al. (1968). The structure refinements were carried out in space group *Pbnm* using the program PROMETHEUS by Zucker et al. (1983), modified by R. Heinemann. Fe and Mg were allowed to occupy the M1 and M2 sites, subject to chemical and site constraints (Table 2). Mn, in the presence of Fe and Mg, strongly prefers the M2 site (Henderson et al. 1996; Redfern et al. 1996). Choosing the simplest assumption, we assigned Mn completely to the M2 site. Neglect of a minor amount of Mn on M1 somewhat affects the value of the equilibrium distribution coefficient, K_D , but leaves the conclusions unaltered. The $|F_o|$ values were weighted according to $w = 1/\sigma^2(|F_o|)$, where $\sigma^2(|F_o|) = \sigma_c^2(|F_o|) + (1/2P|F_o|)^2$ (e.g., Stout and Jensen 1989). $\sigma_c^2(|F_o|)$ is based on counting statistics; P is an instrument instability factor. P was equated with R_i , the $|F|$ based internal agreement of the data (e.g., Le Hénaff et al. 1997). Variation of R_i , as suggested in some refinement programs, was not considered appropriate, because it would bias the weighting scheme towards outliers. Extinction effects were accounted for according to Becker and Coppens (1974) by choosing type I isotropic extinction assuming a Lorentzian mosaic distribution.

Site refinement

Conventional X-ray structure refinements are known to suffer from the inadequacy of the independent, spherically symmetrical atom model (IAM), which ignores the charge redistribution due to chemical bonding. Calculated structure amplitudes satisfactorily reproduce observed values only in the high order (HO) region ($\sin\theta/\lambda < 0.6 \text{ \AA}^{-1}$), whereas they often fail to do so in the low order (LO) region where non-spherically distributed valence electrons, which are not accounted for by the IAM significantly contribute to the scattering. This

deficiency can cause “model outliers” as demonstrated in Figure 1. Maximum $\Delta|F|$ values even approach $12\sigma(|F_o|)$. All outliers are in fact restricted to the LO region whereas outliers due to measurement errors would be expected to be distributed over the whole range of data.

The distribution of the outliers can be modified by varying the valence states of the atoms. However, this cannot remedy the deficiency of the IAM.

High order truncation (HOT) analysis

To investigate the effect that the outliers may have on the results of the site refinements, a bivariate analysis (high order truncation (HOT) analysis) was carried out following the method of Kroll et al. (1997). Starting with the full set of observed structure amplitudes ($\sin\theta/\lambda_{\max} = 1.1 \text{ \AA}^{-1}$), $\sin\theta/\lambda_{\max}$ was

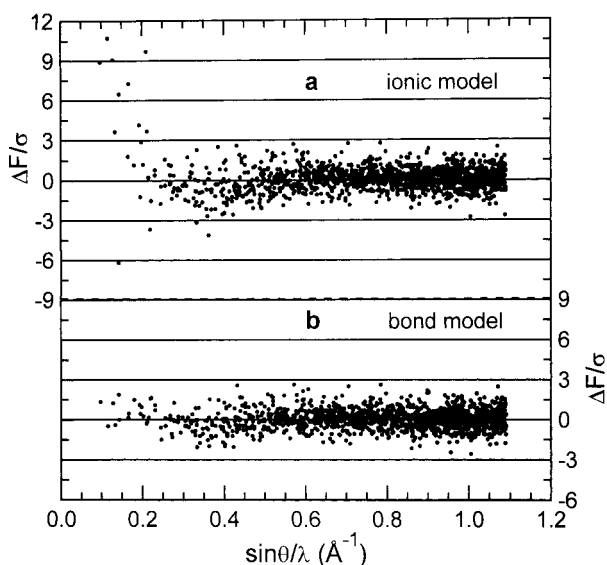


FIGURE 1. Variation with $\sin \theta/\lambda$ of weighted residuals, $\Delta F/\sigma = (|F_o| - |F_c|)/\sigma$, taken from structure refinements using all data on olivine L7 (annealed at 750 °C, and then quenched to room temperature). (a) Refinement based on the independent atom model with all atoms taken as fully ionic. Several model outliers ($\Delta F > 3\sigma$) occur. (b) Refinement based on the “bond model” with all cations taken as fully ionic, oxygen atoms as O^{2-} , and point-charges placed on the Si-O bonds. Model outliers are no longer present. All measured $|F_o|$ values were included in the two refinements.

TABLE 2. Site occupancies X_{Fe}^{M2} : weighted averages from HOT refinements based on the bond model

	R_w (%)*	R_i (%)*	GOF*	X_{Fe}^{M2}	σ (λ)	$\ln(K_D)$	σ [$\ln(K_D)$]
L7 equil. at 750 °C	1.20-1.77	1.14-2.07	0.77-0.81	0.1065	0.0009	0.1561	0.0184
L7 equil. at 650 °C	1.32-1.99	1.14-2.07	0.69-0.70	0.1091	0.0011	0.1055	0.0223
L7 equil. at 500 °C	1.07-1.61	0.92-1.77	0.60-0.62	0.1111	0.0009	0.0650	0.0173
L7 untreated	1.58-1.95	1.35-1.85	0.79-0.96	0.1129	0.0012	0.0297	0.0240
L8 equil. at 750 °C	1.19-1.64	1.08-1.93	0.85-0.95	0.1070	0.0010	0.1462	0.0188
L8 equil. at 650 °C	1.19-1.70	1.11-2.02	0.82-0.91	0.1083	0.0010	0.1207	0.0189
L8 equil. at 500 °C	1.16-1.45	0.98-1.49	0.63-0.76	0.1092	0.0009	0.1034	0.0167
L8 untreated	1.11-1.54	0.99-1.84	0.86-0.98	0.1143	0.0009	0.0028	0.0171

Chemical and site constraints are: $X_{Fe}^{M1} = 0.230 - X_{Fe}^{M2}$, $X_{Mg}^{M1} = 1 - X_{Fe}^{M1}$, $X_{Mg}^{M2} = 0.99 - X_{Fe}^{M2}$, $X_{Mn}^{M2} = 0.01$.

* Ranges are given, see text.

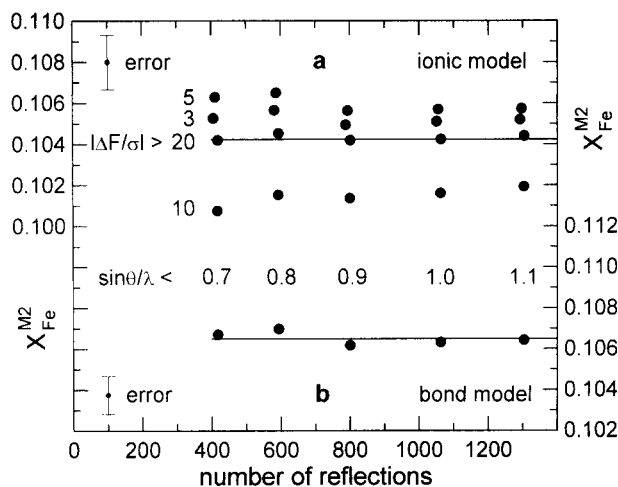


FIGURE 2. High order truncation (HOT) analyses of the set of $|F_o|$ values measured on olivine L7 (750 °C) used in Figure 1. (a) Ionic model: for each $\sin\theta/\lambda$ cut-off, X_{Fe}^{M2} depends on the exclusion criterion $|\Delta F/\sigma|$. (b) Bond model: all $|\Delta F/\sigma| < 3\sigma$, X_{Fe}^{M2} is almost independent of the subset of $|F_o|$ values. Weighted averages of X_{Fe}^{M2} are indicated by the solid lines.

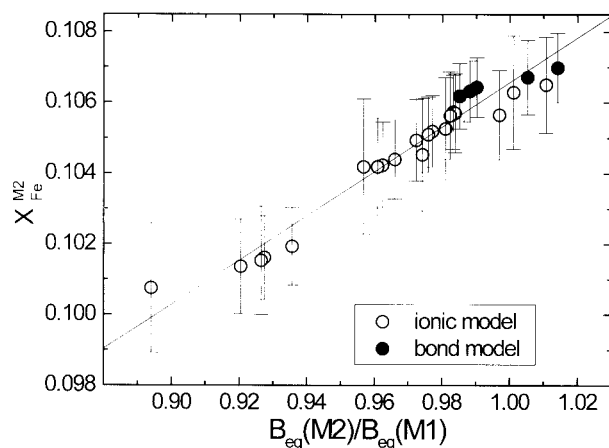


FIGURE 3. Correlation between site occupancy X_{Fe}^{M2} and isotropic temperature factor ratio $B_{eq}(M2)/B_{eq}(M1)$.

reduced in subsequent steps of $0.1/\text{\AA}^{-1}$ down to $0.7/\text{\AA}^{-1}$. These refinements were first carried out employing all reflections of each subset. Next, reflections with $(|F_o| - |F_c|)/\sigma$ exceeding 10, 5, and 3, respectively, were rejected. The resulting 20 site occupancies X_{Fe}^{M2} (Fig. 2a) show their clear dependence on the chosen subset of data.

The data scatter is not restricted to X_{Fe}^{M2} . It is well known that correlations occur between model parameters, in particular between scale factor, extinction coefficient, atomic “vibrational” parameters, and site occupancies. Figure 3 shows the positive correlation between the last two parameter groups (see also Kroll et al. 1997 for a discussion). The effect that an increase in X_{Fe}^{M2} (corresponding to a decrease in X_{Fe}^{M1}) has on calculated structure amplitudes is counterbalanced by an in-

crease in the ratio of “vibrational” parameters of the M2 and M1 sites. This causes an unwanted element of uncertainty to enter the determination of site occupancies. Therefore, one would be more confident if the data scatter in a HOT analysis were small. As is seen below, this can be achieved by reducing the inadequacy of the IAM.

It should be clear that the HOT analysis is not meant to suggest keeping or removing outliers in the course of a refinement. It is merely intended to indicate to what extent site occupancies can depend on different subsets of data, and thus to give an idea to what extent the IAM and the quality of the measured intensity data may bias refined site occupancies.

Bond model

The deficiency of the IAM can be mitigated by two different simple measures.

(1) Kroll et al. (1997) suggested a procedure of bivariate analysis based on stepwise truncation of low-order intensity data. Thereby, bonding electron densities become less and less important and correlation effects can be circumvented by a controlled adjustment of the atomic “vibrational” parameters. (2) Tsirelson et al. (1990) reviewed experimental electron density distributions in silicates and the bond induced charge accumulations on the Si-O bonds. In a simple extension of the IAM, the charge accumulations can be accounted for by placing point charges on the bonds (Kirfel and Will 1980; Vad et al. 1997). The resulting “bond model” has been successfully applied in electron density studies requiring unbiased atomic parameters.

This study follows the second approach. Fully ionized cations were used, oxygen was given a charge of -1 . Charge neutralization was provided by an electron placed midway between each pair of Si and O atoms. The coordinates and anisotropic “vibrational” parameters of the “electrons” were allowed to vary. With this “bond model”, all outliers disappeared (Fig. 1b). This demonstrates that they were not a consequence of measurement errors but were all caused by the IAM model adopted. All $|F_o|$ values are now adequately accounted for. Because all $|\Delta F/\sigma|$ values are less than 3, the number of $|F_o|$ -subsets for the HOT analysis was reduced to the five chosen $\sin\theta/\lambda$ cut-offs. Figure 2b shows that the dependence of the refined site occupancies on the $|F_o|$ -subset is now negligible. Note that we could not detect any correlations between the site occupancies and the bonding-electron parameters ($\gamma_{max} < 0.4$).

Weighted averages of the site occupancies derived from the HOT analyses of the eight data sets of the L7 and L8 crystals using the bond model are listed in Table 2. Similar trends on heat-treated olivines have been found by Aikawa et al. (1985), Ottonello et al. (1990), and Princivalle (1990).

RESULTS

Temperature dependence of the equilibrium Fe,Mg distribution

The temperature variation of the equilibrium distribution coefficient, $K_D = (X_{Fe}^{M1} \cdot X_{Mg}^{M2}) / (X_{Fe}^{M2} \cdot M_{Mg}^{M1})$, is obtained from a weighted regression analysis of the data in Table 2:

$$\ln(K_D) = 0.345(60) - 204(53)/T, \quad (8)$$

where T is in K.

Figure 4 combines the new data with results of in situ neutron scattering experiments on olivine Fa_{12} by Artioli et al. (1995). A similar trend of $K_D(T)$ was also observed for Fa_{50} (Rinaldi et al. 1997). The neutron experiments were performed at vanadium-vanadium oxide buffer conditions using an evacuated vanadium furnace (10^{-5} mbar). Under the assumption that the results derived from two different methods and under different conditions of data collection and refinement can be combined, the following result is obtained: At low temperatures, Fe is predicted to slightly prefer the M2 site. Full disorder is attained at 260–360 °C. At higher temperatures, as was first noted by Smith and Hazen (1973), Fe starts to order onto M1. This is in agreement with the observation that Fe tends to be enriched in the M2 site of (slowly cooled) metamorphic olivines, but in the M1 site of (rapidly cooled) volcanic ones (Aikawa et al. 1985). Above ~880 °C the process of ordering reverts, and full disorder is attained for a second time, at ~900 °C, followed at still higher temperature by a second regime in which Fe prefers M2. Due to the fast Fe,Mg exchange kinetics, a natural olivine would follow the reverse path, with the exchange process freezing in at say 300 °C, i.e., close to full disorder.

The slope of the $\ln(K_D)$ line is very gentle in the region below 750 °C, i.e., the Fe,Mg distribution varies only slightly with temperature. This is most likely the result of a balance between competing forces. Ghose (1982) argues that on the one hand the Fe^{2+} ion prefers the larger M2 site, because Fe^{2+} is larger than Mg^{2+} . On the other hand, Fe^{2+} prefers the smaller, but more distorted M1 site, because the transition metal character of Fe allows a greater degree of covalent bonding with the oxygen ions of M1. In other words, the internal field controlling the Fe,Mg site preference is a complex and non-uniform function of temperature. It vanishes roughly at 300 and 900 °C, and changes drastically at 880 °C. If this is true, the effect can be expected to be reflected by detectable changes in

the structural parameters. It is therefore interesting to obtain more evidence of the high temperature structures of (Fe,Mg) olivines. In situ X-ray experiments are currently in progress.

Olivine: a potential geospeedometer?

The work by Henderson et al. (1996) and Redfern et al. (1996) on $\text{MnMg}[\text{SiO}_4]$ and $\text{MnFe}[\text{SiO}_4]$ tephroites raised hopes that (Fe,Mg) olivines could possibly provide a useful geospeedometer. From the site occupancies of the two untreated crystals which correspond to apparent equilibration temperatures of 325(30) and 375(50) °C one could in principle derive cooling rates. We restrain from this, because it appears that two requirements would have to be fulfilled more closely. First, we need rate constants for the Fe,Mg exchange process that can be more reliably extrapolated to low temperatures than those which can currently be derived from Fe,Mg interdiffusion data. Second, the slope of the $\ln(K_D)$ line is so small that it needs to be even more tightly constrained than presented here (see the 1σ -lines in Fig. 4). This could be achieved by a higher number of data points including those of reversed experiments, and by improved data collection, correction, and evaluation techniques. It is tempting to put effort into that goal because olivines are advantageous compared to orthopyroxenes, because they usually provide a better single crystal quality and suffer less from impurity element concentrations or exsolution products. Finally, restricting such studies to olivines from unweathered meteorites containing metallic Fe, the dependence of the Fe,Mg-exchange rate on oxygen fugacity or total pressure could be safely neglected.

ACKNOWLEDGMENTS

This work was supported by grants given to H. Kroll and A. Kirfel by the Deutsche Forschungsgemeinschaft in the Priority Program "Experimentelle Studien über Elementverteilungen," which is gratefully acknowledged. Our thanks are also due to J. Zipfel, Mainz, for providing the Acapulco samples, and to J. Ganguly, R. Oberti, E. Prince, and S.A.T. Redfern for their constructive reviews.

REFERENCES CITED

- Aikawa, N., Kumazawa, M., and Tokonami, M. (1985) Temperature dependence of intersite distribution of Mg and Fe in olivine and the associated change of lattice parameters. *Physics and Chemistry of Minerals*, 12, 1–8.
- Akamatsu, T. and Kumazawa, M. (1993) Kinetics of intracrystalline cation redistribution in olivine and its implication. *Physics and Chemistry of Minerals*, 19, 423–430.
- Artioli, G., Rinaldi, R., Wilson, C.C., and Zanazzi, P.F. (1995) High-temperature Fe-Mg cation partitioning in olivine: In-situ single-crystal neutron diffraction study. *American Mineralogist*, 80, 197–200.
- Becker, P.J. and Coppens, P. (1974) Extinction within the limit of validity of the Darwin transfer equations. I. General formalism for primary and secondary extinction and their application to spherical crystals. *Acta Crystallographica*, A30, 129–147.
- Bocquet, J.L., Brébec, G., and Limoge, Y. (1983) Diffusion in metals and alloys. In R.W. Cahn and P. Haasen, Eds., *Physical Metallurgy* (3rd edition), p. 385–475. North-Holland Physics Publishing, Amsterdam.
- Buening, D.K. and Buseck, P.R. (1973) Fe-Mg lattice diffusion in olivine. *Journal of Geophysical Research*, 78, 6852–6862.
- Chakraborty, S. (1997) Rates and mechanisms of Fe-Mg interdiffusion in olivine at 980–1300 °C. *Journal of Geophysical Research*, 102, 12317–12331.
- Ganguly, J. and Tazzoli, V. (1994) Fe^{2+} -Mg interdiffusion in orthopyroxene: Retrieval from the data on intracrystalline exchange reaction. *American Mineralogist*, 79, 930–937.
- Ghose, S. (1982) Mg-Fe order-disorder in ferromagnesian silicates. I. Crystal Chemistry. In S.K. Saxena, Ed., *Advances in Physical Geochemistry*, Vol. 2, p. 4–57. Springer, New York.
- Henderson, C.M.B., Knight, K.S., Redfern, S.A.T., and Wood, B.J. (1996) High-temperature study of cation exchange in olivine by neutron powder diffraction.

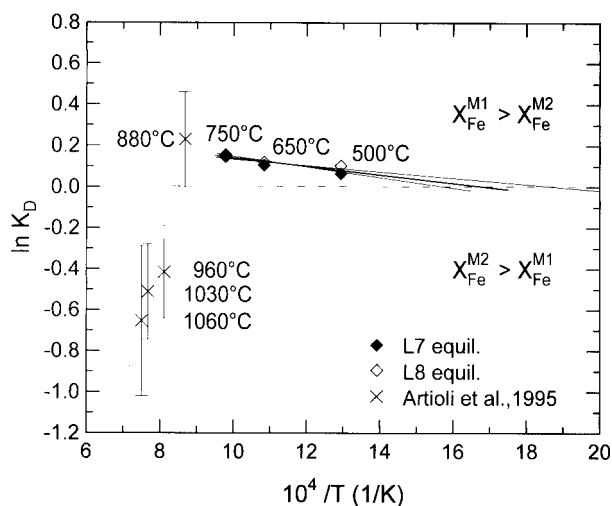


FIGURE 4. Variation of $\ln(K_D)$ with temperature. The two bracketing lines indicate the 1σ -uncertainty.

- Science, 271, 1713–1715.
- Jurewicz, A.J.G. and Watson, E.B. (1988) Cations in olivine, Part 2: Diffusion in olivine xenocrysts, with applications to petrology and mineral physics. *Contributions to Mineralogy and Petrology*, 99, 186–201.
- Kirfel, A. (1996) Cation distributions in olivines and orthopyroxenes. An interlaboratory study. *Physics and Chemistry of Minerals*, 19, 503–519.
- Kirfel, A. and Will, G. (1980) Bonding in $[\text{S}_2\text{O}_6]^{2-}$. Refinement and pictorial representation from an X-ray diffraction study of $\text{Na}_2\text{S}_2\text{O}_6 \cdot 2\text{H}_2\text{O}$ and $\text{Na}_2\text{S}_2\text{O}_6 \cdot 2\text{D}_2\text{O}$. *Acta Crystallographica*, B36, 512–523.
- Kroll, H., Lueder, T., Schlenz, H., Kirfel, A., and Vad, T. (1997) The Fe^{2+} , Mg distribution in orthopyroxene: A critical assessment of its potential as a geospeedometer. *European Journal of Mineralogy*, 9, 705–733.
- Le Hénaff, C., Hansen, N.K., Protas, J., and Marnier, G. (1997) Electron Density Distribution in LiB_3O_5 at 293 K. *Acta Crystallographica*, B53, 870–879.
- Misener, D.J. (1974) Cationic diffusion in olivine to 1400 °C and 35 kbar. In A.W. Hofmann, B.J. Gilotti, H.S. Yoder Jr., and R.A. Yund, Eds., *Geochemical Transport and Kinetics*, p. 117–129. Carnegie Institution of Washington, Washington, D.C.
- Mueller, R.F. (1967) Model for order-disorder kinetics in certain quasi-binary crystals of continuously variable composition. *Journal of Physics and Chemistry of Solids*, 28, 2239–2243.
- (1969) Kinetics and thermodynamics of intracrystalline distributions. *Mineralogical Society of America, Special Paper*, 2, 83–93.
- North, A.C.T., Phillips, D.C., and Mathews, F.S. (1968) A semi-empirical method of absorption correction. *Acta Crystallographica*, A24, 351–359.
- Ottonello, G., Princivalle, F., and Della Giusta, A. (1990) Temperature, composition, and f_{O_2} effects on intersite distribution of Mg and Fe^{2+} in olivines. *Physics and Chemistry of Minerals*, 17, 301–312.
- Princivalle, F. (1990) Influence of temperature and composition on Mg- Fe^{2+} intracrystalline distribution in olivines. *Mineralogy and Petrology*, 43, 121–129.
- Redfern, S.A.T., Henderson, C.M.B., Wood, B.J., Harrison, R.J., and Knight, K.S. (1996) Determination of olivine cooling rates from metal-cation ordering. *Nature*, 381, 407–409.
- Rinaldi, R., Artioli, G., Henderson, C.M.B., Redfern, S.A.T., Wood, B.J., and Knight, K.S. (1997) Octahedral cation ordering in Fe,Mg olivines as a function of temperature and composition. *European Union of Geosciences, Abstract Supplement No. 1, Terra Nova*, 9, 426.
- Stout, G.H. and Jensen, L.H. (1989) X-ray structure determination (second edition), pp. 453. A Wiley-Interscience Publication, New York.
- Tsirelson, V.G., Evdokimova, O.A., Belokoneva, E.L., and Urusov, V.S. (1990) Electron density distribution and bonding in silicates. A review of recent data. *Physics and Chemistry of Minerals*, 17, 275–292.
- Vad, T., Kirfel, A., Schlenz, H., and Kroll, H. (1997) Neue Verfeinerungen zur (Fe,Mg)-Kationenverteilung in einem synthetischen Orthopyroxen. *Beihefte zum European Journal of Mineralogy*, 9, 367.
- Zipfel, J., Palme, H., Kennedy, A.K., and Hutcheon, D. (1995) Chemical composition and origin of the Acapulco Meteorite. *Geochimica et Cosmochimica Acta*, 59, 3607–3627.
- Zucker, U.H., Perenthaler, E., Kuhs, W.F., Bachmann, R., and Schulz, H. (1983) A program system for sophisticated structure refinement. *Max-Planck Institut für Festkörperforschung, Stuttgart*.

MANUSCRIPT RECEIVED JUNE 9, 1998

MANUSCRIPT ACCEPTED MAY 21, 1999

MANUSCRIPT HANDLED BY ROBERTA OBERTI